

This is a pre print version of the following article:

3D human foreskin model for testing topical formulations of sildenafil citrate / Magnano, Greta Camilla; Quadri, Marika; Palazzo, Elisabetta; Lotti, Roberta; Loschi, Francesca; Dall'Acqua, Stefano; Abrami, Michela; Larese Filon, Francesca; Marconi, Alessandra; Hasa, Dritan. - In: INTERNATIONAL JOURNAL OF PHARMACEUTICS. - ISSN 0378-5173. - 649:(2024), pp. 123612-123623. [10.1016/j.ijpharm.2023.123612]

Terms of use:

The terms and conditions for the reuse of this version of the manuscript are specified in the publishing policy. For all terms of use and more information see the publisher's website.

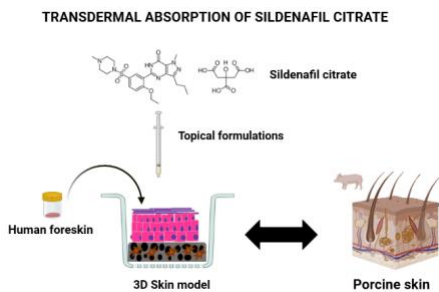
31/05/2026 21:12

(Article begins on next page)

4 ABSTRACT

5 Sildenafil citrate is an effective and approved drug used for the treatment of erectile dysfunction and
6 premature ejaculation. Despite a widespread application, sildenafil citrate shows a low oral
7 bioavailability that brings to a delayed onset of action, and numerous adverse cardiovascular effects in
8 high-risk patients. For these reasons, local transdermal drug delivery of this drug is being explored as
9 an interesting and noninvasive alternative administration method that avoids adverse effects arised from
10 peak plasma drug concentrations. Although human and animal skin represents the most reliable models
11 to perform penetration studies, they involve a series of ethical issues and restrictions. For these reasons
12 new *in vitro* approaches based on artificially reconstructed human skin or “human skin equivalents” are
13 being developed as possible alternatives for transdermal testing. There is little information, however, on
14 the efficiency of such new *in vitro* methods on cutaneous penetration of active ingredients. The objective
15 of the current study was to investigate the sildenafil citrate loaded in three commercial transdermal
16 vehicles using 3D full-thickness skin equivalent and compare their permeability ability with the porcine
17 skin. Our results demonstrated that, while the formulation plays an imperative role in an appropriate
18 dermal uptake of sildenafil citrate, the D coefficient results obtained by using the 3D skin equivalent are
19 comparable to those obtained by using the porcine skin when a simple drug suspension is applied (1.17
20 $\times 10^{-10} \pm 0.92 \times 10^{-10} \text{ cm}^2/\text{s}$ vs $3.5 \times 10^2 \pm 3.3 \times 10^2 \text{ cm}^2/\text{s}$), suggesting that in such case, this 3D skin
21 model can be a valid alternative for *ex-vivo* skin absorption experiments.

22 GRAPHICAL ABSTRACT



23

24 **Key words:** 3D human skin equivalent; permeability; porcine skin; sildenafil citrate; formulations

25 1. INTRODUCTION

26 Erectile dysfunction (ED) is the inability to maintain and/or attain the erectile state of the penis allowing
27 for sufficient and satisfactory sexual intercourse (Lue et al. 2004). This common clinical disorder has
28 been thought to affect up to 52% of males aged between 40 to 70 years (Feldman et al. 1994). Sildenafil
29 citrate (Viagra®, Pfizer, New York, NY, USA) is an effective and approved molecule used for the
30 treatment of erectile dysfunction (Fink et al. 2002); (Salonia, Rigatti, et Montorsi 2003); (Badwan et al.
31 2001); (Kirby, Creanga, et Stecher 2013). This drug allows corpus cavernosum smooth muscle to relax,
32 potentiating erections during sexual stimulation, by selectively inhibiting phosphodiesterase type 5
33 (PDE5) (Ghofrani, Osterloh, et Grimminger 2006); (Langtry et Markham 1999) ; (Thompson et al.
34 2001). Specifically, the primary mechanism of action of sildenafil involves the inactivation of cyclic
35 guanosine monophosphate (cGMP), the downstream mediator of the vasodilating agent nitric oxide
36 (NO) resulting in smooth muscle relaxation in penile cavernous tissues (Moreland, Goldstein, et Traish
37 1998); (Andersson et Wagner 1995); (Lau et Adaikan 2006). Sildenafil is rapidly absorbed after oral
38 administration and the time to achieve maximal peak plasma concentration varies from 0.5 to 2 hours
39 (De Toni et al. 2018). Due to its poor solubility, however, sildenafil shows a low oral bioavailability
40 (38– 41%) that brings to a delayed onset of action, and possible adverse interactions with other drug
41 such as cardiovascular and hypertension effects in high-risk patients (Muirhead et al. 2002); (Osman, El
42 Maghraby, et Hedaya 2006); (Zinner 2007). In the last 15-20 years, many studies focused on the safety
43 of sildenafil following oral administration, and raised some issues including cardiovascular deaths in
44 patients, and in some cases suggesting that the treatment with this drug needs to be stopped immediately
45 (Kloner 2000); (Tran et Howes 2003); (Kontaras, Varnavas, et Kyriakides 2008); (Tracqui et al. 2002).
46 For such reasons, cutaneous application of the citrate salt of sildenafil has been proposed as a
47 noninvasive alternative method (Atipairin et al. 2020) ; (Abdelalim, Abdallah, et Elnaggar 2020); (Y. S.
48 R. Elnaggar, Massik, et Abdallah 2011); (Badr-Eldin et Ahmed 2016); (Y. Elnaggar, El-Massik, et
49 Abdallah 2011); (Akula et P.K. 2018); (Farghali et Ahmed 2015). .However, despite the increasing
50 number of studies where several formulations for the transdermal administration of sildenafil have been
51 proposed, studies focusing on the skin permeability of such molecule are missing. In recent years,
52 various *in vitro* models using synthetic skin membranes have been introduced and investigated to rapidly

53 screen the passive transport of a specific molecule through a given membrane (Kansy, Senner, et
54 Gubernator 1998). The parallel artificial membrane permeation assay (PAMPA) showed a positive
55 correlation between the permeability of various compounds through such membrane and human skin
56 (Ottaviani, Martel, et Carrupt 2006). Similarly, Magnano et al. (Magnano, Sut, et al. 2022) demonstrated
57 that the permeability of [6]-gingerol following exposure to ginger pure extract using skin mimicking
58 barrier (SMB) was comparable to those obtained by using the porcine skin, suggesting that the new
59 barrier can be a good alternative to *ex-vivo* animal skin for conducting percutaneous penetration
60 experiments. Today, new *in vitro* approaches based on artificially reconstructed human skin or “human
61 skin equivalents (HSE)” are being developed as possible alternative sources of tissue for skin permeation
62 experiments (Neupane et al. 2020); (Iliopoulos, Chapman, et Lane 2021); (Suhail et al. 2019);
63 (Westmoreland et Holmes 2009). HSE is three-dimensional (3D) *in vitro* tissue-engineered human skin,
64 constructed by culturing human keratinocytes and fibroblasts using sophisticated technologies and
65 quality systems (Idrees et al. 2021). These 3D models are physiologically more similar to the native
66 human skin in terms of morphology, lipid composition, differentiation markers (Ponec et al. 2002);
67 (Ponec et al. 2000); (Netzlaff et al. 2005), and functionality (viability and metabolism) with respect to
68 *ex vivo* human tissues (Bell et al. 1981), representing a highly predictive and reproducible instrument
69 for preclinical evaluations. Moreover, these advanced 3D models allow to study tumors, including
70 malignant melanoma (MM) as reported by Marconi (Marconi et al. 2018), due to their ability to provide
71 an excellent microenvironment that is closer to the *in vivo* situation to investigate the progression and
72 invasion of the tumor, reducing time-consuming associated to animal studies, and to be cost-effective.
73 HSEs are designed to comprise either only the epidermis or both the dermis and epidermis (full-
74 thickness HSEs) (Zhang et Michniak-Kohn 2012). Currently, *in vitro* commercially available 3D models
75 are epidermal-only models, including EpiSkin™, EpiDerm™, and SkinEthic™. The use of HSEs have
76 been validated or are under validation as alternative to animal testing methods for the evaluation of
77 chemical and ingredient hazard: skin irritation (OCED TG 439), skin corrosion (OECD TG 431), eye
78 irritation and skin sensitization (EURL ECVAM Status Report on the Development, Validation and
79 Regulatory Acceptance of Alternative Methods and Approaches (2015) and skin absorption
80 experiments (OECD 2004). It is also worth mentioning that the permeability of molecules through 3D

81 skin models is much higher compared to those measured in human skin *ex vivo*, due to less well-
82 developed barriers (Huong et al. 2009). Nevertheless, these skin equivalent models clearly show higher
83 reproducibility of data, reducing the variability between replicates, which is typically present in skin
84 permeation studies using human or animal skin tissues due to the inter-individual and intra-individual
85 (according to site) variations. Interestingly, such 3D skin models seemed to correctly predict the
86 percutaneous absorption rank order of a series of compounds with different physicochemical properties
87 (Van Gele et al. 2011); (Doucet, Garcia, et Zastrow 1998); (Gay et al. 1992); (Michel et al. 1995);
88 (Dreher et al. 2002). The validation and implementation of these experimental models as alternative
89 methods in the evaluation of the molecule permeation, therefore, are strongly promoted, representing a
90 promising scientific innovation. The first aim of this work was to study the skin penetration of sildenafil
91 citrate loaded in three commercial transdermal formulations as model vehicles using 3D full-thickness
92 skin equivalent. The second aim was to compare preliminary permeation assays through the new 3D
93 human foreskin model with skin permeation experiments performed using Franz's diffusion cells and
94 porcine ear skin as model membrane, in order to examine 3D full-thickness skin equivalent as useful
95 membrane for transdermal studies. To further support the good comparability between 3D full-thickness
96 skin equivalent and porcine skin we also performed the diffusion experiments of a sildenafil citrate
97 solution (standard aqueous sample). The choice of sildenafil citrate as a model drug to evaluate the 3D
98 model was dictated for several reasons namely (i) our interest on the use of topical formulations as an
99 alternative administration method for penile treatment (ii) at our knowledge the current study represents
100 the first example where the skin penetration of sildenafil citrate is investigated using a 3D human skin
101 equivalent obtained from human foreskin (iii) sildenafil citrate is often preferred to pure sildenafil in
102 commercial formulations for its superior water solubility. .

103 2. MATERIAL AND METHODS

104 2.1. MATERIALS

105 All chemicals used in this study were of analytical grade. Specifically, acetonitrile (ACN), ethanol, and
106 formic acid were purchased from Sigma-Aldrich (St. Louis, Missouri, USA). Sodium chloride, sodium
107 hydrogenphosphate, and potassium dihydrogenphosphate were obtained from Carlo Erba (Milan, Italy).

108 Water (reagent grade) was produced with a Millipore purification pack system (MilliQ water). The
109 physiological solution used as the receptor fluid was prepared by dissolving 2.38 g of Na₂HPO₄, 0.19 g
110 of KH₂PO₄ and 9 g of NaCl into 1 liter of MilliQ water (final pH = 7.35). Dulbecco's Modified Eagle's
111 Medium (DMEM), Ham's F12 and Gold Keratinocyte Basal Medium (KBM) were purchased from
112 Lonza, (Basel, Switzerland); Fetal bovine serum (FBS), Penicillin/Streptomycin/Amphotericin (PSA);
113 L-Glutamine; DMEM/HAM'SF12 composed of insulin (5 µg/mL); transferrin (5 µg/mL),
114 triiodothyronine (2 nM), cholera enterotoxin (0.1 nM), hydrocortisone (0,4 µg/mL), adenine (180 nM)
115 epidermal growth factor (10 ng/mL) from Sigma-Aldrich (Missouri, USA).

116 2.2. PREPARATION OF THREE MODEL TOPICAL FORMULATIONS OF SILDENAFIL 117 CITRATE

118 In order to check the role of formulation on the permeability, sildenafil citrate was incorporated in three
119 preformed commercial transdermal used as model vehicles, and were purchased from Fagron Italia S.r.l.
120 (Bologna, Italy). The composition of the selected model formulations is shown in Table 1. Specifically,
121 formulations A and B are liposomal creams with B being more lipophilic, while formulation C is a
122 classic o/w cream. The three formulations were selected since all contain different enhancers such as
123 such isopropyl myristate and isopropyl palmitate (formulation A), short chain alcohols and glycols
124 (formulation B) or olive oil and oleic acid (formulation C) and thus can potentially accelerate the
125 cutaneous permeation of sildenafil citrate (Lane 2013); (Williams et Barry 2004). The dispersion of the
126 active into each formulation was performed through the following procedure: approximately 1.950 mg
127 of sildenafil citrate was added to 25 mL of a specific vehicle (formulation A, B or C) and transferred in
128 30 mL container. The mixture was stirred using an unguator (Gako unguator, Farmalabor, Italy) for 6
129 minutes at 1000 rpm. The resulting product was stored at room temperature. To determine the
130 concentration of sildenafil citrate in each formulation, 0.5 mL of each topic cream (corresponding to a
131 theoretical amount of 38.6 mg of sildenafil citrate) was dissolved in 6.0 mL of 50/50 % (v/v)
132 water/ethanol solution. The sample was stirred for 4 hours, filtered through a 0.45 µm polypropylene
133 housing, polytetrafluoroethylene (PTFE) membrane filter (Whatman®) and assayed by HPLC, using a

134 method reported in the paragraph 2.7. The experimental amounts of the active in 0.5 mL of formulations
 135 A, B and C were 31.30 ± 1.11 mg, 31.25 ± 1.74 mg and 31.44 ± 0.99 mg, respectively.

136 Table 1 : List of the selected formulations and information given by the manufactures in the label related to composition.

FORMULATION	INGREDIENTS
Formulation A	Sildenafil citrate, water, isopropyl myristate, glyceryl monostearate, PEG-40 stearate, stearic acid, isopropyl palmitate, lecithin, simethicone, urea, cetyl alcohol, stearyl alcohol, potassium sorbate E202, benzoic acid, EDTA, butylated hydroxytoluene (BHT), sorbic acid, carbomer, hydrochloric acid E507.
Formulation B	Sildenafil citrate, water, soybean lecithin, caprylic/capric triglyceride, sorbitol, dimethicone, propylen glycol, stearyl alcohol, glyceryl stearate, alcohol, cetearyl alcohol, cetearth-20, PEG-100 stearate, cetyl esters wax, octyldodecanol, steareth-2, steareth-21, phenoxyethanol, hydroxyethyl acrylate/sodium acryloyldimethyl taurate copolymer, ethylhexylglycerin, magnesium aluminum silicate
Formulation C	Sildenafil citrate, water, glycerine, C12 -15 alkyl benzoate, glyceryl stearate, PEG-100 stearate, stearic acid, oleic acid, olive oil, phenoxyethanol, dimethicone, hydroxyethyl acrylate/sodium acryloyldimethyl taurate copolymer, caprylic/capric triglyceride, cetyl alcohol, trolamine, tocopheryl acetate, ethylhexylglycerin

137 2.3. RHEOLOGICAL PROPERTIES

138 Rheological properties of the three topical formulations were determined using a stress controlled
 139 rotational rheometer (Haake Mars Rheometer, 379-0200 Thermo Electron GmbH, Karlsruhe, Germany)
 140 equipped with plate-plate geometry (PP60, diameter= 60 mm) and a Peltier temperature control system.
 141 Samples were loaded between devices and all measurements were carried with a fixed gap of 0.5 mm.
 142 Viscoelastic properties of the products were analyzed through several rheological tests. Flow experiment
 143 was performed at constant temperature $T=25^{\circ}\text{C}$, over a range shear rate of 1 to 1000 s^{-1} . Temperature
 144 sweep was carried from 5 to 40°C at a heating rate of $1^{\circ}\text{C}/\text{min}$ and an oscillation frequency of 1 Hz.
 145 Time sweep was evaluated for 120s at a fixed frequency and temperature (1 Hz and 37°C , respectively).
 146 Mechanical spectra were obtained using frequency sweep from 0.1 to 100 Hz at 37°C .

147 2.4. 3D HUMAN SKIN EQUIVALENT

148 2.4.1. ISOLATION OF PRIMARY HUMAN FIBROBLASTS

149 Primary human dermal fibroblasts (hDF) were obtained from foreskins of two different individuals.
 150 Samples were collected with written informed consent of patients, according to the Declaration of
 151 Helsinki after approval of the Modena Medical Ethical Committee (Prot. 184/10). Isolated cells were

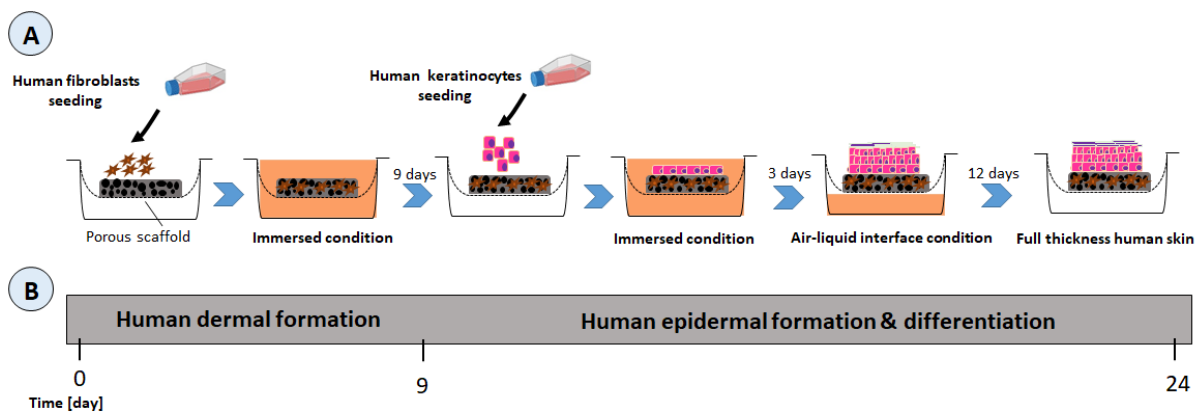
152 cultured in 175-cm² flasks as described by Lotti (Lotti et al. 2022) at 37°C in a 5 % CO₂ humidified
153 atmosphere and 95% air incubator. Cell culture medium was Dulbecco's modified Eagle medium
154 (DMEM), supplemented with 5% (v/v) fetal bovine serum (FBS), 2% (v/v) Glutamine, 1% (v/v)
155 Penicillin-Streptomycin-Amphotericin (PSA). The medium was exchanged every 2 days. Fibroblasts
156 were used for up to 8 passages (P8), reaching 70-80% confluency.

157 2.4.2. ISOLATION OF PRIMARY HUMAN EPIDERMAL KERATINOCYTES

158 Primary human epidermal keratinocytes (hEK) were isolated from foreskins according to the Modena
159 Medical Ethical Committee (Prot. 184/10) and seeded onto murine 3T3 fibroblasts, as feeder layers.
160 Cells were cultured in 75-cm² flasks in Ham's F12 medium/Dulbecco's modified Eagle medium
161 (DMEM), containing 10% (v/v) fetal bovine serum (FBS), penicillin (100 U/mL), streptomycin (0.1
162 mg/mL), Glutamine (4 mM), supplemented with a cocktail of adenine (0.18 mM), insulin (5 µg/mL),
163 transferrin (5 µg/mL), hydrocortisone (0.4 µg/mL), triiodothyronine (2 nM), cholera enterotoxin (0.1
164 nM), epidermal growth factor (10 ng/mL). The medium was exchanged every 2 days. Keratinocytes
165 were used at low passage (P2) and subcultured at confluency between 70 and 80%.

166 2.4.3. 3D RECONSTRUCTED HUMAN SKIN EQUIVALENT

167 The 3D fully-human skin equivalent was generated by successively fabricating a dermal compartment
168 consisting of fibroblasts and a multi-layered, well differentiated epidermal compartment on top of the
169 dermis as summarized in Figure 1. Polystyrene scaffolds (12-well Alvetex[®] scaffold inserts,
170 REPROCELL Europe Ltd, Glasgow, UK) were used for the development of 3D skin equivalent,
171 following the protocol described by Zoio (Zoio 2022). In the 12-well insert format, the scaffold has a
172 diameter of 15 mm and an effective area of 1.12 cm². The thickness of the 3D skin equivalent was 200
173 µm.



174

175 Figure 1 : (A) Schematic representation of the methodology for the development of 3D fully human skin equivalent (HSE). It is generated
 176 using a porous polystyrene scaffold seeded with fibroblasts to recreate the dermal layer. Then keratinocytes are seeded on top of the dermal
 177 layer and the culture is raised to air liquid interface culture conditions to allow the keratinocytes to differentiate and form epidermal layers.
 178 (B) : Timeline for the development of HSE.

179 2.5. PORCINE EAR SKIN PREPARATION

180 Porcine skin was used as a skin model in the penetration test due to its similarity in terms of morphology
 181 and permeability to human skin (Schmook, Meingassner, et Billich 2001); (Barbero et Frasc 2009);
 182 (Wester et al. 1998); (Simon et Maibach 2000). Piglet ears were collected immediately after the
 183 suppression of the animal and stored at -25°C on aluminum foil for a period of up to 4 months. On the
 184 day of the experiment, the piglet ears were thawed in a physiological solution at room temperature and
 185 the skin samples were cut into 4 cm^2 square pieces. The thickness of the skin samples used was measured
 186 with a micrometric caliper (Mitutoyo, Roissy en France, France), obtaining an average value of $0.97 \pm$
 187 0.03 mm . To evaluate skin integrity, Trans Epidermal Water Loss (TEWL) was measured on each skin
 188 piece after one hour of equilibration using a Vapometer (Delfin Vapometer, Delfin Technologies,
 189 Sweden) already used in our previous work (Magnano, Marussi, et al. 2022): the average TEWL values
 190 of skin samples was found to be below $10\text{ g}\cdot\text{m}^{-2}\cdot\text{h}^{-1}$ (Guth et al. 2015).

191 2.6. *IN-VITRO* ABSORPTION STUDIES

192 2.6.1. PERMEATION ASSAY OF SILDENAFIL CITRATE THROUGH 3D FULL SKIN 193 EQUIVALENT

194 The permeation test for sildenafil citrate from three topical formulations (formulation A, formulation B
 195 and formulation C) was investigate and compared with the aqueous suspension of the drug. 3D skin
 196 equivalents ($200\text{ }\mu\text{m}$) were transferred into a new six-well plate, where skin penetration study was

197 conducted. The receptor (basolateral)/surrounding compartment was filled with 4.5 mL of physiological
198 solution, touching the tissue from below. The effective skin area for diffusion was 1.12 cm². At time 0
199 (beginning of the experiment), 0.5 mL of each formulation (The experimental amount of the active in
200 0.5 mL of each formulation is reported in section 2.2) was carefully applied on the surface of the skin
201 equivalent. This resulted in a theoretical applied dose of sildenafil citrate $Q_0 = 34.5 \text{ mg/cm}^2$. The plate
202 was subsequently covered, horizontally shaken and maintained at 32°C, 5% CO₂, throughout the
203 experiment (4 h). At pre-specified time intervals (0, 20, 40, 60, 120, 180, and 240 min) 1.0 mL of
204 receptor solution was withdrawn and immediately replaced with an equal volume of fresh buffer.
205 Samples were analyzed by high performance liquid chromatography (HPLC). Experiments were
206 conducted in three replicates.

207 2.6.2. PERMEATION AND RETENTION STUDY OF SILDENAFIL CITRATE 208 THROUGH PORCINE SKIN

209 Skin absorption studies were performed in static diffusion cells according to the OECD guidelines
210 (OECD 2004). The skin pieces were mounted between the donor and receptor chamber of Franz-type
211 static diffusion cells with the *stratum corneum* facing the donor chamber. The effective skin area for
212 diffusion was 0.95 cm². The receptor fluid (RF) was composed of a physiological solution that was
213 continuously stirred using a Teflon coated magnetic stirrer. The concentration of the salt in the receptor
214 fluid is approximately the same as that found in the blood. The receptor compartment had a mean volume
215 of 4.5 mL filled with RF. Mounted Franz cells were maintained at $32 \pm 1^\circ\text{C}$ by means of circulation of
216 thermostated water in the jacket surrounding the cell. At time 0, 0.5 mL of formulation A (corresponding
217 to 38.6 mg of sildenafil citrate) were accurately deposited in direct contact with the porcine skin surface
218 in the Franz cell. This resulted in a theoretical applied dose of sildenafil citrate $Q_0 = 40.6 \text{ mg/cm}^2$. To
219 assess the absorption experiments, formulation A was selected and was compared with that from drug
220 aqueous suspension. The permeation study lasted 4 hours, in order to determine the permeation profile
221 of sildenafil citrate remaining and permeating through the skin. At selected time points (0, 20, 40, 60,
222 120, 180, and 240 min) 1.0 mL of each receptor sample was collected and analyzed. An equal volume
223 of fresh receptor fluid was immediately replaced in each sample in order to maintain sink conditions.

224 All the experiments were conducted on 3 independent biological replicates. The amounts of sildenafil
225 citrate in RF as well as in each skin layer after 4 hours were quantified by HPLC (see later section 2.7)

226 2.6.3. COLLECTION AND TREATMENT OF SAMPLES

227 Ear skin piece was washed three times with 1.0 mL of MilliQ. For each biological sample the *stratum*
228 *corneum* (SC) was isolated from viable layers by tape stripping (4 strips) using D-Squame tape
229 (Monaderm, Monaco) and placed in vials each containing 4.0 mL of MilliQ and stirred for 4 hours.
230 Subsequently, the explant epidermis and dermis (E+D) were cut into small pieces with a scalpel, then
231 immersed in 4.0 mL of MilliQ, stirred for 4 hours and diluted 1:10 in MilliQ before HPLC analysis.
232 Sildenafil citrate was extracted from each fraction (*stratum corneum*, epidermis + dermis) at room
233 temperature for 4 hours. After each extraction, aliquots of 1.0 mL were filtered through a 0.45 μm
234 polypropylene filter (polytetrafluoroethylene (PTFE) membrane filter, Whatman[®] Maidstone, United
235 Kingdom) before analysis by UV-HPLC. Three replicates were performed for each experiment.

236 2.7. ANALYSIS OF SILDENAFIL CITRATE BY HIGH PERFORMANCE LIQUID 237 CHROMATOGRAPHY (HPLC)

238 For each test, the concentration of sildenafil citrate was obtained using an Agilent 1260 chromatograph
239 (Santa Clara, CA, USA) equipped with a diode array (DAD). Agilent InfinityLab Poroshell 120 C18
240 (3.0 \times 100 mm, 4.0 μm) was used as stationary phase, with temperature set to 23°C. The mobile phase
241 was composed of acetonitrile (A) and 0.1% formic acid water (B), in gradient elution mode, at a flow
242 rate of 0.4 mL/min, in isocratic phase: 30% A, 70% B. The injection volume was 10 μL , and the detection
243 wavelength was 254 nm. The retention time of sildenafil citrate was at 4.8 ± 0.02 min and the total run
244 time was 8 min. Limit of quantification (LOQ) and limit of detection (LOD) were 0.12 $\mu\text{g}/\text{mL}$ and 0.04
245 $\mu\text{g}/\text{mL}$ respectively.

246 2.8. PERMEABILITY CALCULATIONS AND DATA ANALYSIS

247 The cumulative amount of permeated drug (dQ, expressed in μg) was plotted as a function of time (dt
248 expressed in s). The linear portion of the slope, corresponding to the steady-state (Hopf et al. 2020) was
249 utilized to calculate the flux according to Eq. 1.

250
$$J = \frac{dQ}{A \cdot dt} \quad (1)$$

251 Where A represents the surface area of the barrier (expressed in cm²). The calculated flux was used to
252 calculate the apparent permeability coefficient (P_{app}) as Eq. (2):

253
$$P_{app} = \frac{J}{C_d} \quad (2)$$

254 where P_{app} (cm/s) is the apparent permeability coefficient, J (μg/cm² per s) is the flux at the steady state
255 and C_d is the drug donor concentration (μg/cm³). The lag time (t_{lag}) that is the delay time of the first
256 contact of the drug with the skin's surface until a steady state flux is established was calculated as the
257 intercept of the plots. In the simplest case of Fickian diffusion through a homogeneous membrane of
258 thickness (h) t_{lag} is given by Eq. (3) (Hopf et al. 2020)

259
$$t_{lag} = \frac{h^2}{6D} \quad (3)$$

260 Furthermore, the diffusion coefficient (D, units of cm²/s) was calculated utilizing Eq. 4 (Hopf et al.
261 2020)

262
$$D = \frac{h^2}{t_{lag} \cdot 6} \quad (4)$$

263 2.9. HISTOLOGICAL ANALYSIS

264 The reconstructed tissues were fixed with formalin for 2 hours at room temperature, dehydrated, and
265 embedded in paraffin wax to allow for transverse sectioning. Sections were thinly sliced (4 μm thick)
266 using a microtome and these were stained using a hematoxylin and eosin (H&E) stain kit (Vector
267 Laboratories Inc., Burlingame, CA, USA). Staining times were 5 min for hematoxylin and 1 min for
268 eosin. The H&E stained slides were examined with a D-Sight slide scanner (Menarini Diagnostics,
269 Bagno a Ripoli, Firenze, Italy). The thickness of the 3D skin equivalent was measured using ImageJ
270 software (National Institutes of Health, Bethesda, MD, USA) in 6 microscope fields.

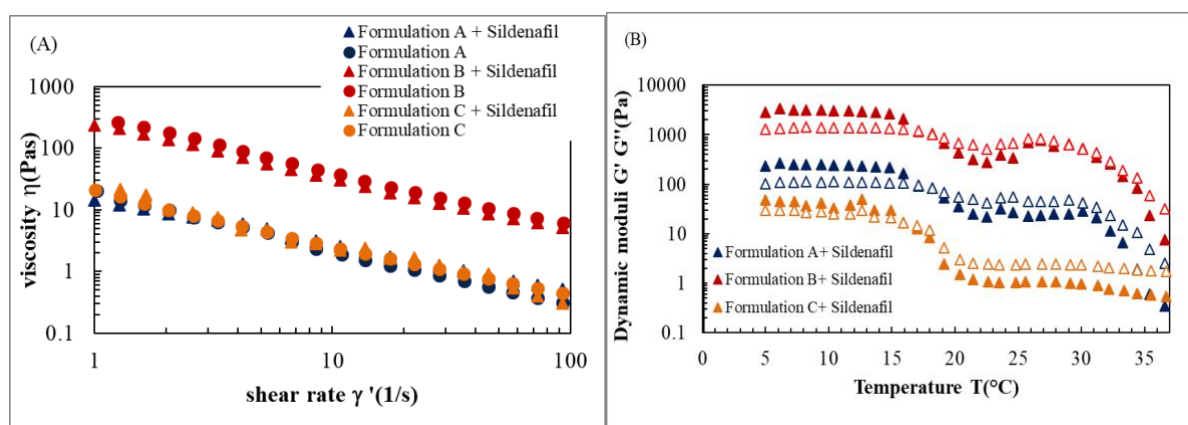
271 2.10. STATISTICAL ANALYSIS

272 The results are expressed as the quantity permeated per skin surface unit ($\mu\text{g}/\text{cm}^2$). Data from skin
273 absorption experiments were expressed as mean \pm standard deviation (SD). Statistical analysis of
274 differences between two groups were analyzed by Student t-test and those between multiple groups were
275 performed using the analysis of variance (ANOVA, one-way) The significance level was set at $p < 0.05$.

276 3. RESULTS

277 3.1. CHARACTERIZATION OF THE CREAMS: RHEOLOGICAL PROPERTIES

278 The rheological properties of the three topical bases in which sildenafil citrate was dispersed are reported
279 in Figure 2. The flow curve and temperature sweep of all the samples present a classical shear thinning
280 behavior with viscosity dropping down by increasing the shear rate. The loading process and the
281 presence of the drug in the formulation did not alter the rheological properties of the bases. However,
282 formulation B presented higher viscosity compared to A and C, possibly due to structural differences
283 between the tested products.



284
285 Figure 2 : (A) Flow curve of formulations A(blue), B(red) and C(orange) with and without Sildenafil (triangle and circles respectively) ; (B)
286 temperature sweep of formulations A(blue), B(red) and C(orange) with drugs, G' was reported with close symbols, G'' with open symbols.

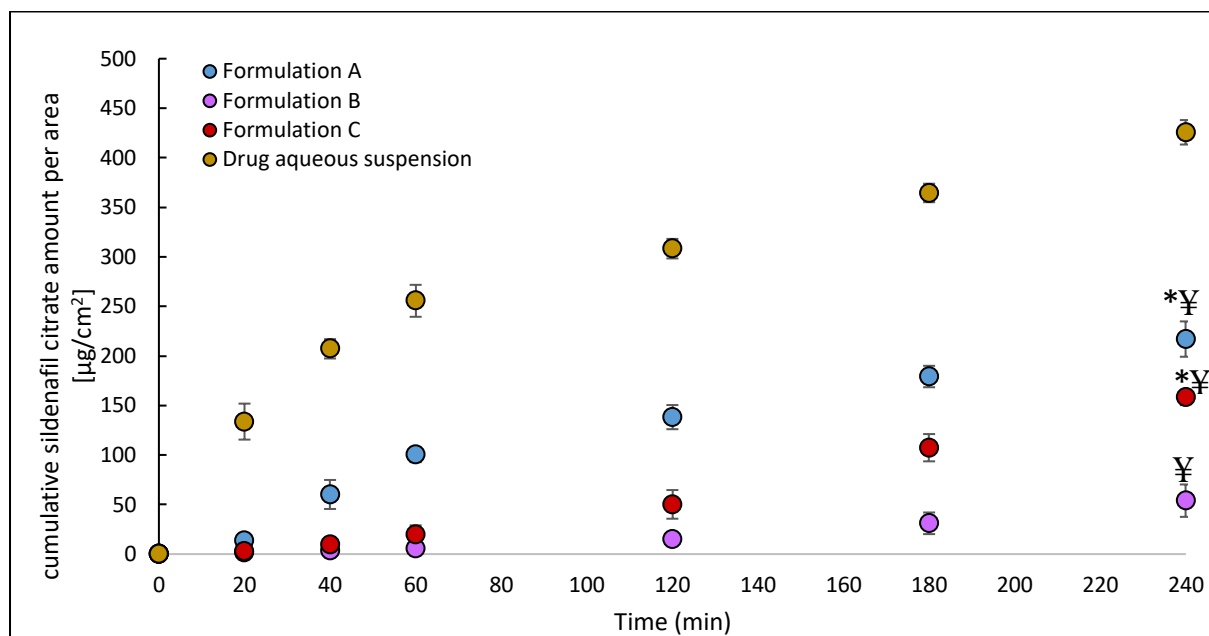
287 The temperature sweep plot in Figure 2B showed the formulation dependence on heating. Also in this
288 case, all formulations showed similar behaviour although each formulation presented different values
289 of dynamic moduli. Going into more details, at 5 $^{\circ}\text{C}$ elastic moduli G' were slightly higher than the
290 viscous ones G'' , indicating a transition state between solid ($G' \gg G''$) and liquid ($G' \ll G''$) behaviour.
291 The real transition where G'' clearly overcame G' occurred at around 18 $^{\circ}\text{C}$ and systems remained in the

292 sol phase at higher temperatures. The results reported in Figure 2 are in agreement with data reported in
293 the literature (Pharmaceutics 2020, 12, 105). Finally, similar to the viscosity results reported in Figure
294 2A, formulation B showed higher G values compare to the other two formulations.

295 3.2. PERMEATION PROFILES OF SILDENAFIL CITRATE FROM NEW TOPICAL 296 FORMULATIONS THROUGH 3D SKIN EQUIVALENTS

297 The concentrations of sildenafil citrate loaded into three basic topical formulations and the aqueous
298 suspension in the 3D skin equivalents are reported in Figure 3. It can be observed that the amount of
299 drug in the basolateral medium increase over time among all the formulations at the end of the contact
300 time (4 hours). Notably, the sildenafil citrate from the aqueous suspension showed the highest
301 permeation profile reaching a concentration of $426 \pm 12.3 \mu\text{g}/\text{cm}^2$ after 4 hours suggesting that the
302 molecule can easily cross the 3D full thickness skin when available in solution. This is an important
303 result confirming that the strategy of the local administration of this molecule is possible. Certainly, a
304 simple aqueous suspension of the sildenafil citrate cannot be suitable for local application, but rather it
305 must be incorporated in appropriate formulations with optimal rheological properties that can release
306 the active with a desired profile. A topical product requires optimization also in terms of texture and
307 affinity. In this context, among the three topical formulations, the amount of sildenafil citrate was
308 particularly high in formulation A and formulation C after 4 h of contact through 3D full-thickness skin
309 samples ($217 \pm 17.8 \mu\text{g}/\text{cm}^2$ and $165 \pm 13.3 \mu\text{g}/\text{cm}^2$, respectively), while the maximum concentration of
310 the drug reached in the formulation B was $53.9 \pm 28.3 \mu\text{g}/\text{cm}^2$. A statistically significant difference
311 between drug aqueous suspension and the three topical formulations was found. Importantly, the
312 different RF data of sildenafil citrate at 4 h, obtained by formulation B and the other two creams are
313 also statistically different. However, steady state transdermal flux of sildenafil citrate was found to be
314 close and in the same order of magnitude only for formulation C and formulation A through 3D skin
315 models, ranging from $1.96 \times 10^{-4} \pm 0.76 \times 10^{-4} \mu\text{g}/\text{cm}^2 \cdot \text{s}$ to $2.05 \times 10^{-4} \pm 0.12 \times 10^{-4} \mu\text{g}/\text{cm}^2 \cdot \text{s}$, and 1 to
316 2 times higher than those obtained for formulation B ($0.69 \times 10^{-4} \pm 0.38 \times 10^{-4} \mu\text{g}/\text{cm}^2 \cdot \text{s}$ $p < 0.05$, Table
317 2). The P_{app} (cm/s) of sildenafil citrate from each formulation through 3D skin model was determined
318 dividing the flux at the steady state by the concentration of sildenafil citrate in the donor solution (C_d)

319 (see experimental section 2.8). The drug suspension exhibited the highest value of P_{app} ranging around
 320 $9.05 \times 10^{-9} \pm 0.89 \times 10^{-9}$ cm/s, while formulation A and formulation C showed similar values of P_{app}
 321 ($5.30 \times 10^{-9} \pm 0.30 \times 10^{-9}$ cm/sec and $5.08 \times 10^{-9} \pm 2.56 \times 10^{-9}$ cm/s, respectively). On the other hand the
 322 lowest value of P_{app} was registered for formulation B ($1.79 \times 10^{-9} \pm 0.99 \times 10^{-9}$ cm/s) (Table 2).



323
 324 Figure 3 : Sildenafil citrate amount ($\mu\text{g}/\text{cm}^2$) from topical formulations and from aqueous suspension that permeated in the receptor fluid at
 325 specific extraction times through 3D full thickness skin. Values are expressed as mean \pm standard error of the mean (SEM) ($n=3$). (¥) show
 326 the statistically significant differences obtained between aqueous suspension and topical formulations $p < 0.05$. Asterisk (*) indicates
 327 statistically significant differences between formulation B and the other two tested formulations (formulation A and formulation C; $p < 0.05$).

328 Table 2: Flux (J), apparent permeability coefficients (P_{app}) and sildenafil citrate concentration loaded into three basic topical formulations
 329 and from the aqueous suspension measured for 3D full thickness skin. Values are expressed as mean \pm SD ($n=3$). (¥) show the statistically
 330 significant differences obtained between aqueous suspension and topical formulations $p < 0.05$. Asterisk (*) indicates statistically significant
 331 differences between formulation B and the other two tested formulations (formulation A and formulation C; $p < 0.05$).

Formulation	J ($\mu\text{g}/\text{cm}^2 \cdot \text{s}$)	P_{app} (cm/s)	Sildenafil citrate concentration in RF at 4 h ($\mu\text{g}/\text{cm}^2$)
Drug aqueous suspension	$2.87 \times 10^{-4} \pm 0.28 \times 10^{-4}$	$9.05 \times 10^{-9} \pm 0.89 \times 10^{-9}$	426 ± 12.3
Formulation A	$2.05 \times 10^{-4} \pm 0.12 \times 10^{-4} * ¥$	$5.30 \times 10^{-9} \pm 0.30 \times 10^{-9} * ¥$	$217 \pm 30.9 * ¥$
Formulation B	$0.69 \times 10^{-4} \pm 0.38 \times 10^{-4} ¥$	$1.79 \times 10^{-9} \pm 0.99 \times 10^{-9} ¥$	$53.9 \pm 28.3 ¥$
Formulation C	$1.96 \times 10^{-4} \pm 0.76 \times 10^{-4} * ¥$	$5.08 \times 10^{-9} \pm 2.56 \times 10^{-9} * ¥$	$165 \pm 13.3 * ¥$

332

333 3.3. PERMEATION OF SILDENAFL CITRATE THROUGH PORCINE EAR SKIN MODEL

334 To examine the 3D full skin equivalent as a new skin model for skin penetration of molecules,

335 permeation experiments were assessed using porcine ear skin through Franz cell method. Among the

336 three topical creams, formulation A was selected due to its suitable rheological behavior leading to a

337 better release profile of the active thus a higher permeability, observed through 3D skin model. Diffusion

338 experiments of a sildenafil citrate suspension (standard aqueous sample) was also performed. The

339 concentrations of sildenafil citrate from formulation A and from drug water suspension that passed into

340 the receptor per unit area of skin are reported in Figure 4. Sildenafil citrate permeated through the two

341 skin models, showing the following trend: 3D full skin equivalent drug suspension > 3D full skin

342 equivalent formulation A > porcine ear skin drug suspension > porcine ear skin formulation A (Figure

343 4). Specifically, the mean amount of sildenafil citrate from formulation A observed in RF at the end of

344 the contact time (4 hours) were $217 \pm 30.9 \mu\text{g}/\text{cm}^2$ for the 3D full skin equivalent samples and $42.4 \pm$

345 $24 \mu\text{g}/\text{cm}^2$ when porcine ear skin was used. Similarly, the content of sildenafil citrate from aqueous

346 suspension through 3D full skin equivalent samples was higher than those obtained for porcine ear skin

347 ($426 \pm 12.3 \mu\text{g}/\text{cm}^2$ and $358 \pm 189 \mu\text{g}/\text{cm}^2$, respectively). As it can be seen the different RF data of

348 sildenafil citrate at 4h, obtained by 3D skin equivalent and the other biological membrane are statistically

349 different. Steady state transdermal fluxes of sildenafil citrate from formulation A and from aqueous

350 suspension through 3D equivalent skin models, however, were found to be 2 times higher than those

351 obtained for porcine ear skin (formulation A : $2.05 \times 10^{-4} \pm 0.12 \times 10^{-4} \mu\text{g}/\text{cm}^2 \cdot \text{s}$ vs $0.57 \times 10^{-4} \pm 0.33$

352 $\times 10^{-4} \mu\text{g}/\text{cm}^2 \cdot \text{s}$ $p < 0.05$; drug suspension $2.87 \times 10^{-4} \pm 0.28 \times 10^{-4} \mu\text{g}/\text{cm}^2 \cdot \text{s}$ vs $0.99 \times 10^{-4} \pm 0.89 \times$

353 $10^{-4} \mu\text{g}/\text{cm}^2 \cdot \text{s}$ $p < 0.05$ Table 3). The P_{app} (cm/s) of sildenafil citrate through each skin model was

354 determined dividing the flux by the concentration of sildenafil citrate in the donor solution (C_d) (see

355 experimental section 2.8). 3D full skin equivalent produced the highest values of P_{app} ranging around

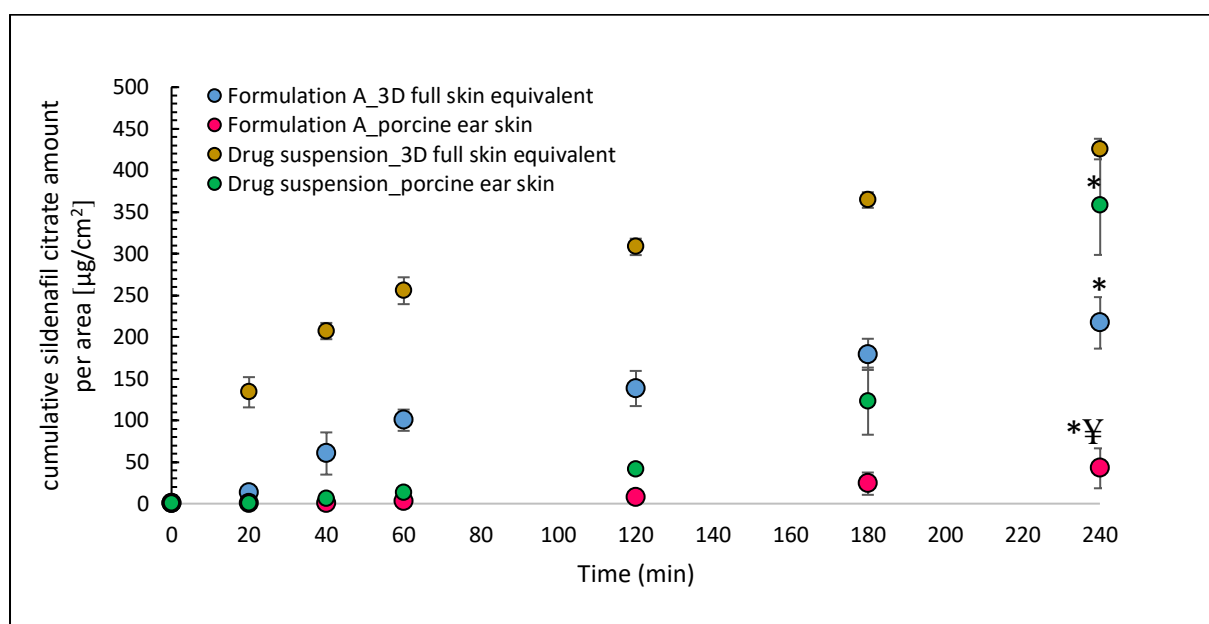
356 $5.30 \times 10^{-9} \pm 0.30 \times 10^{-9} \text{ cm/s}$ for formulation A and $9.05 \times 10^{-9} \pm 0.89 \times 10^{-9} \text{ cm/s}$ for drug suspension

357 compared to those measured through porcine ear skin ($1.48 \times 10^{-9} \pm 0.86 \times 10^{-9} \text{ cm/s}$ and $3.16 \times 10^{-9} \pm$

358 $3.09 \times 10^{-9} \text{ cm/s}$, respectively) (Table 3). Importantly, the different diffusion coefficients of the aqueous

359 suspensions of sildenafil citrate obtained by 3D skin equivalent and the porcine skin are $1.17 \times 10^{-10} \pm$

360 0.92×10^{-10} cm/s and $3.5 \times 10^2 \pm 3.3 \times 10^2$ cm/s, respectively ($p=0.105$). The differences between the
 361 two models remain statistically not significant, showing that the two tested models are comparable. On
 362 the other hand, the D coefficient of formulation A calculated for porcine ear skin was $5.3 \times 10^2 \pm 0.29 \times$
 363 10^2 cm/s, while $1.06 \times 10^{-10} \pm 0.06 \times 10^{-10}$ cm/s was obtained for 3D skin equivalent ($p=0.005$) (Table 3).
 364 It is important to underline that a statistically significant difference between the porcine skin and the 3D
 365 skin equivalent was found, demonstrating that the two models are not comparable when semisolid
 366 products are applied as the case of formulation A.



367
 368 Figure 4 : Sildenafil citrate amount from formulation A and from drug aqueous suspension ($\mu\text{g}/\text{cm}^2$) that permeated in the receptor fluid at
 369 specific extraction times through porcine ear skin and 3D full thickness skin. Values are expressed as mean \pm SD (n=3). (¥) show the statistically
 370 significant differences obtained between formulation A through 3D skin equivalent and porcine skin $p < 0.05$. Asterisk (*) indicates statistically
 371 significant differences between drug suspension through 3D full thickness skin and the other samples ($p < 0.05$).

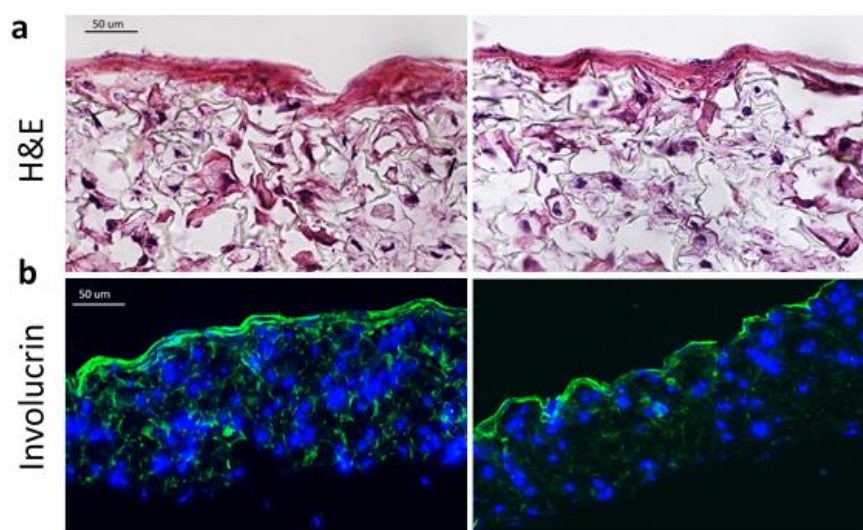
372 Table 3: Flux (J), apparent permeability coefficients (P_{app}), diffusion coefficients (D) and sildenafil citrate concentration loaded in vehicle A
 373 and from aqueous suspension measured for each skin model. Values are expressed as mean \pm SD (n=3). (¥) show the statistically significant
 374 differences obtained between formulation A through 3D skin equivalent and porcine skin $p < 0.05$. Asterisk (*) indicates statistically
 375 significant between drug suspension through 3D skin equivalent and the other samples ($p < 0.05$).

Model	J ($\mu\text{g}/\text{cm}^2 \cdot \text{s}$)	P_{app} (cm/s)	D (cm^2/s)	Sildenafil citrate concentration in RF at 4 h ($\mu\text{g}/\text{cm}^2$)
3D full skin equivalent formulation A	$2.05 \times 10^{-4} \pm 0.12 \times 10^{-4} *$	$5.30 \times 10^{-9} \pm 0.30 \times 10^{-9} *$	$1.06 \times 10^{-10} \pm 0.06 \times 10^{-10} *$	$217 \pm 30.9 *$
3D full skin equivalent drug suspension	$2.87 \times 10^{-4} \pm 0.28 \times 10^{-4}$	$9.05 \times 10^{-9} \pm 0.89 \times 10^{-9}$	$1.17 \times 10^{-10} \pm 0.92 \times 10^{-10}$	426 ± 12.3

Porcine ear skin formulation A	$0.57 \times 10^{-4} \pm 0.33 \times 10^{-4} \text{**}\text{¥}$	$1.48 \times 10^{-9} \pm 0.86 \times 10^{-9} \text{**}\text{¥}$	$5.3 \times 10^2 \pm 0.29 \times 10^2$	$42.4 \pm 24 \text{**}\text{¥}$
Porcine ear skin drug suspension	$0.99 \times 10^{-4} \pm 0.89 \times 10^{-4} \text{*}$	$3.16 \times 10^{-9} \pm 3.09 \times 10^{-9} \text{*}$	$3.5 \times 10^2 \pm 3.3 \times 10^2$	$358 \pm 189 \text{*}$

376 3.4. MORPHOLOGICAL ANALYSIS OF 3D SKIN EQUIVALENT

377 The morphology of the developed skin equivalent was analyzed by conducting H&E staining on
378 transverse sections. Figure 5 shows that the 3D model formed a skin complex architecture with a
379 complete epidermis, mimicking the normal process of epidermal stratification and resembling what has
380 been previously described by Zoio (Zoio 2022). Moreover, the expression of involucrin, critically
381 involved in the formation of the cornified cell envelope, was evaluated to analyze the epidermal barrier
382 formation in the skin equivalent. The results reveal the presence of such typical epidermal tissue protein
383 in the skin equivalent, confirming the epidermal differentiation (Figure 5).



384
385 Figure 5 : Hematoxylin and Eosin staining of the 3D full thickness skin equivalent. (a): The morphology of the developed skin equivalent. (b):
386 Expression of involucrin. The corresponding bright field image. Scale bar: 50 µm

387 4. DISCUSSION

388 Pure sildenafil possesses limited water solubility due to its hydrophobic nature and it is classified as
389 Biopharmaceutics Classification System (BCS) class II drug (Kim et al. 2019). As a consequence, the
390 citrate salt form is often preferred in commercial formulation for its superior water solubility (Sawatdee
391 et al. 2019); (Doghri et al. 2019); (Renshall et al. 2020). Moreover, the salt form is able to guarantee
392 transdermal absorption when administered cutaneously. Indeed, our data demonstrated that the highest

393 amount of sildenafil citrate permeated through 3D skin equivalent was registered for the aqueous drug
394 suspension (Figure 3 and Table 2). This might be justified by the fact that drug suspension on the skin
395 surface would provide a layer of more concentrated solution in skin pores resulting in higher
396 concentration gradient and increased permeation with time. These results support the choice of the salt
397 form for topical applications and transdermal absorption of sildenafil. The results reported in Figure 3
398 and Table 2 showed also the importance of formulation compositions on skin absorption. Among the
399 three topical vehicles, formulation A presented the highest skin permeation of sildenafil citrate. Such
400 observation can be related to the liposomal structure of such formulation that has been already
401 demonstrated to improve transdermal absorption of drugs (Egbaria et Weiner 1990); (Shigeta et al.
402 2004); (Rahimpour et Hamishehkar 2012). A similar permeation rate was observed when sildenafil
403 citrate was dissolved in the oil-in-water (o/w) emulsion formulation C, which is also an appropriate
404 system for topical application (Otto, du Plessis, et Wiechers 2009), allowing the penetration of
405 hydrophilic substances through the *stratum corneum* of the skin (Hoppel et al. 2015). Moreover, it is
406 generally presumed that the penetration of ingredients in an o/w emulsion is higher when they are
407 dissolved in the continuous phase of the emulsion (Wiechers 2005). Since in a typical o/w emulsion the
408 ingredients are mainly distributed into the water continuous phase (Otto, du Plessis, et Wiechers 2009)
409 it may be hypothesized that the affinity of sildenafil citrate for some ingredients of formulation C in the
410 continuous phase of the emulsion can apparently facilitate the dermal uptake. An additional reason for
411 the enhanced skin penetration of sildenafil citrate from formulation C can be related to the increase in
412 the hydration level of the *stratum corneum*, caused by exposure to the external aqueous phase of such
413 water-rich emulsion (Otto, du Plessis, et Wiechers 2009). Moreover, the positive effect of formulation
414 C may be due to the presence of the olive oil, which act as transdermal enhancer affecting the permeation
415 pathway of the drug (Čižinauskas et al. 2017); (Alhasso, Ghorri, et Conway 2022). Conversely, the skin
416 permeation of sildenafil citrate from formulation B was much lower compared to the other two tested
417 creams (Figure 3 and Table 2). This may be attributed to the fact that formulation B is a liposomal
418 organogel (lipophilic gel) representing a difficult vehicle for sildenafil citrate to diffuse and eventually
419 cross the skin. Indeed, such formulation presented higher viscosity compare to the other products (Figure
420 2). Generally, a highly viscous cream shows low spreadability on the skin, while low viscosity eases the

421 application; in fact, it was reported in the literature a correlation between low viscosity of a vehicle and
422 faster skin penetration of the incorporated drug (Kogan et Garti 2006). In this work, we explored the
423 potential application of an *in vitro* 3D-human skin equivalent (3D-HSE) as an alternative method to
424 animal and human testing for assessment of dermal uptake of sildenafil citrate. 3D-HSE was generated
425 by fabricating the dermal and epidermal compartments (Figure 1) using primary human cells
426 (keratinocytes and fibroblasts) obtained from healthy donors. Cells growing in 3D tissue cultures have
427 different cell surface receptor expression, proliferative capacity, extracellular matrix synthesis, cell
428 density, and metabolic functions that mimic closely the original human tissue (Brohem et al. 2011).
429 Therefore, skin equivalents should recreate the layers characteristic of the native epidermis: stratum
430 corneum (SC), stratum granulosum (SG), stratum spinosum (SS), and stratum basale (SB) on top of the
431 mature dermis, mimicking the structural and functional properties of native skin as closely as possible
432 (Schäfer-Korting et al. 2008). The *stratum corneum*, is considered as the rate-limiting step for passive
433 drug diffusion across the skin (Scheuplein 1965). Such 3D skin models are preferred in preliminary
434 pharmaceutical studies due to their relative reproducibility, as well as controllable passive transport
435 characteristics (Guenou et al. 2009); (Suhail et al. 2019); however, they can also show some limitations
436 including complexity, high cost and the inability to sustain long-term cell culture (Suhail et al. 2019).
437 To compare preliminary permeation assays through this proposed 3D fully-human skin model, the
438 formulation A of sildenafil citrate prepared and the drug suspension were used for assessing the
439 permeation assays through this 3D skin model in comparison to porcine skin in order to examine 3D
440 full-thickness skin equivalent as useful membrane for transdermal studies. The flux values of sildenafil
441 citrate loaded in vehicle A obtained for 3D full thickness skin equivalent was found to be significantly
442 higher compared to those measured for porcine ear skin (Figure 4 and Table 3). Moreover, the lag time
443 (t_{lag}), the time necessary to establish a linear concentration profile across the barrier was also calculated.
444 Formulation A through porcine ear skin showed a t_{lag} of 93.3 ± 5.1 min, while for 3D skin equivalent
445 the permeation was too rapid and it was not possible to determine t_{lag} . To further support the good
446 comparability between 3D full-thickness skin equivalent and porcine skin we also perform the diffusion
447 experiments of a sildenafil citrate solution (standard aqueous sample). Our results demonstrated higher
448 permeation of drug aqueous suspension through the 3D skin model compared to porcine skin (Figure 4,

449 Table 3). Similarly, the t_{lag} of drug suspension through the 3D skin equivalent was not possible to
450 determine due to the too fast permeation, while the t_{lag} through porcine ear skin was 62.3 ± 59.3 min.
451 However, the diffusion coefficients of drug suspension measured with the 3D full thickness skin
452 equivalent and the porcine ear skin are not statistically different, showing that the two tested models are
453 comparable (Table 3). **On the other hand**, when a more complex system is applied such as formulation
454 A, the D values calculated for 3D skin model and porcine skin are statistically different and in such case
455 these two models don't show a positive correlation. The diffusion coefficient (also known as diffusivity)
456 is an essential parameter to understand the passive diffusion through biological barriers and, as a
457 consequence, bioavailability and biodistribution of an active pharmaceutical ingredient (API) (di Cagno
458 et al. 2018). Furthermore, to develop a suitable skin equivalent as valid substitution for drug permeation,
459 the skin barrier function of this model should be similar to *in vivo* healthy human skin. Epidermis barrier
460 formation is associated with involucrin, a cell envelope protein, expressed at an early stage of
461 keratinocyte differentiation (Steven et Steinert 1994). (Candi, Schmidt, et Melino 2005). This epidermal
462 tissue protein is normally seen only in the upper spinous and granular layers and it promotes envelope
463 formation and cellular cohesion (Candi, Schmidt, et Melino 2005); (Steinert et Marekov 1997). For such
464 reason, the expression of involucrin at its correct anatomical position was verified in order to
465 demonstrate the terminal differentiation of epidermis. The histological evaluation confirms the presence
466 of such typical epidermal tissue protein in our skin model, suggesting the formation of the skin barrier
467 function (Figure 5). Thus, this good correlation should be attributed to the anatomical characteristics of
468 this 3D skin model generated from foreskins. So based on the evidence, we can conclude that when a
469 simple water drug suspension is applied, such skin models are similar. Finally, it is important to point
470 out that further investigations need to be performed, including an increase of the batches cells and a
471 wider range of test molecules such as lipophilic compounds as well as other substances with varying
472 physicochemical properties.

473 5. CONCLUSION

474 Our findings demonstrated that the 3D skin equivalent has a positive correlation with ear porcine skin
475 when simple drug suspensions are applied. On the other hand, for more complex and viscous systems

476 such as formulation A, the two tested skin model cannot be considered comparable. Furthermore it is
477 important to point out the similar anatomical structure of the 3D skin equivalent generated from
478 foreskins with the histological and physiological properties of ear skin barrier. Additionally, the results
479 reported in this study confirmed the importance of the formulation on the dermal permeation of the
480 sildenafil citrate. Although further studies need to be performed, including an expanded panel of
481 substances and pharmaceutical dosage forms, the 3D skin equivalent adopted in this work is able to
482 provide a rapid initial estimation of the amount of sildenafil citrate permeated through the skin, with the
483 potential of being a valid alternative to *ex-vivo* animal skin for skin penetration measurements of new
484 dermal formulations of such important drug.

485 CONFLICT OF INTEREST STATEMENT

486 The authors have no conflict of interest to disclose.

487 AUTHOR CONTRIBUTIONS

488 **Greta Camilla Magnano:** Conceptualization, Data Curation, Investigation, Writing - original draft.
489 **Marika Quadri:** Data Curation, Investigation, Writing - review & editing. **Elisabetta Palazzo:**
490 Investigation, Resources, Writing - review & editing. **Roberta Lotti:** Investigation., Writing - review
491 & editing. **Francesca Loschi:** Investigation. **Stefano Dall'Acqua:** Investigation. **Michela Abrami:**
492 Investigation. **Francesca Larese Filon:** Funding acquisition, Resources. **Alessandra Marconi:**
493 Supervision, Resources, Writing - review & editing. **Dritan Hasa:** Conceptualization, Supervision,
494 Writing - review & editing.

495 REFERENCES

- 496 Abdelalim, Lamiaa R., Ossama Y. Abdallah, et Yosra S.R. Elnaggar. 2020. « High Efficacy, Rapid Onset
497 Nanobiosomes of Sildenafil as a Topical Therapy for Erectile Dysfunction in Aged Rats ». *International Journal of Pharmaceutics* 591 (décembre): 119978.
498 <https://doi.org/10.1016/j.ijpharm.2020.119978>.
499
500 Akula, Pranitha, et Lakshmi P.K. 2018. « Effect of pH on weakly acidic and basic model drugs and
501 determination of their ex vivo transdermal permeation routes ». *Brazilian Journal of*
502 *Pharmaceutical Sciences* 54 (2). <https://doi.org/10.1590/s2175-97902018000200070>.
503 Alhasso, Bahjat, Muhammad Usman Ghori, et Barbara R. Conway. 2022. « Systematic Review on the
504 Effectiveness of Essential and Carrier Oils as Skin Penetration Enhancers in Pharmaceutical
505 Formulations ». *Scientia Pharmaceutica* 90 (1): 14.
506 <https://doi.org/10.3390/scipharm90010014>.

507 Andersson, K. E., et G. Wagner. 1995. « Physiology of Penile Erection ». *Physiological Reviews* 75 (1):
508 191-236. <https://doi.org/10.1152/physrev.1995.75.1.191>.

509 Atipairin, Apichart, Charisopon Chunchachaichana, Titpawan Nakpheng, Narumon Changsan, Teerapol
510 Srichana, et Somchai Sawatdee. 2020. « Development of a Sildenafil Citrate Microemulsion-
511 Loaded Hydrogel as a Potential System for Drug Delivery to the Penis and Its Cellular
512 Metabolic Mechanism ». *Pharmaceutics* 12 (11): 1055.
513 <https://doi.org/10.3390/pharmaceutics12111055>.

514 Badr-Eldin, Shaimaa, et Osama Ahmed. 2016. « Optimized Nano-Transfersomal Films for Enhanced
515 Sildenafil Citrate Transdermal Delivery: Ex Vivo and in Vivo Evaluation ». *Drug Design,
516 Development and Therapy*, avril, 1323. <https://doi.org/10.2147/DDDT.S103122>.

517 Badwan, A, L Nabuls, M Alomari, N Daraghme, et M Ashour. 2001. « Sildenafil Citrate ». In *Profiles
518 of Drug Substances, Excipients and Related Methodology*, 27:339-76. Elsevier.
519 [https://doi.org/10.1016/S0099-5428\(08\)60717-0](https://doi.org/10.1016/S0099-5428(08)60717-0).

520 Barbero, Ana M., et H. Frederick Frasch. 2009. « Pig and Guinea Pig Skin as Surrogates for Human in
521 Vitro Penetration Studies: A Quantitative Review ». *Toxicology in Vitro* 23 (1): 1-13.
522 <https://doi.org/10.1016/j.tiv.2008.10.008>.

523 Bell, Eugene, H. Paul Ehrlich, David J. Buttle, et Takako Nakatsuji. 1981. « Living Tissue Formed in
524 Vitro and Accepted as Skin-Equivalent Tissue of Full Thickness ». *Science* 211 (4486): 1052-54.
525 <https://doi.org/10.1126/science.7008197>.

526 Brohem, Carla A., Laura B. da Silva Cardeal, Manoela Tiago, María S. Soengas, Silvia B. de Moraes
527 Barros, et Silvy S. Maria-Engler. 2011. « Artificial Skin in Perspective: Concepts and
528 Applications: Artificial Skin ». *Pigment Cell & Melanoma Research* 24 (1): 35-50.
529 <https://doi.org/10.1111/j.1755-148X.2010.00786.x>.

530 Cagno, Massimiliano Pio di, Fabrizio Clarelli, Jon Våbenø, Christina Lesley, Sokar Darsim Rahman,
531 Jennifer Cauzzo, Erica Franceschinis, Nicola Realdon, et Paul C. Stein. 2018. « Experimental
532 Determination of Drug Diffusion Coefficients in Unstirred Aqueous Environments by
533 Temporally Resolved Concentration Measurements ». *Molecular Pharmaceutics* 15 (4):
534 1488-94. <https://doi.org/10.1021/acs.molpharmaceut.7b01053>.

535 Candi, Eleonora, Rainer Schmidt, et Gerry Melino. 2005. « The Cornified Envelope: A Model of Cell
536 Death in the Skin ». *Nature Reviews Molecular Cell Biology* 6 (4): 328-40.
537 <https://doi.org/10.1038/nrm1619>.

538 Čižinauskas, Vytis, Nicolas Elie, Alain Brunelle, et Vitalis Briedis. 2017. « Skin Penetration
539 Enhancement by Natural Oils for Dihydroquercetin Delivery ». *Molecules* 22 (9): 1536.
540 <https://doi.org/10.3390/molecules22091536>.

541 De Toni, Luca, Maurizio De Rocco Ponce, Erica Franceschinis, Stefano Dall'Acqua, Roberto Padriani,
542 Nicola Realdon, Andrea Garolla, et Carlo Foresta. 2018. « Sublingual Administration of
543 Sildenafil Oro-dispersible Film: New Profiles of Drug Tolerability and Pharmacokinetics for
544 PDE5 Inhibitors ». *Frontiers in Pharmacology* 9 (février): 59.
545 <https://doi.org/10.3389/fphar.2018.00059>.

546 Doghri, Yosra, Fabien Chetaneau, Moez Rhimi, Aicha Kriaa, Valérie Lalanne, Chantal Thorin,
547 Emmanuelle Maguin, M. Yassine Mallem, et Jean-Claude Desfontis. 2019. « Sildenafil Citrate
548 Long-Term Treatment Effects on Cardiovascular Reactivity in a SHR Experimental Model of
549 Metabolic Syndrome ». Édité par Frank T. Spradley. *PLOS ONE* 14 (11): e0223914.
550 <https://doi.org/10.1371/journal.pone.0223914>.

551 Doucet, O, N Garcia, et L Zastrow. 1998. « Skin Culture Model: A Possible Alternative to the Use of
552 Excised Human Skin for Assessing In Vitro Percutaneous Absorption ». *Toxicology in Vitro* 12
553 (4): 423-30. [https://doi.org/10.1016/S0887-2333\(98\)00023-X](https://doi.org/10.1016/S0887-2333(98)00023-X).

554 Dreher, Frank, Frédéric Fouchard, Claire Patouillet, Michèle Andrian, Jean-Thierry Simonnet, et
555 Florence Benech-Kieffer. 2002. « Comparison of Cutaneous Bioavailability of Cosmetic
556 Preparations Containing Caffeine or α -Tocopherol Applied on Human Skin Models or Human
557 Skin Ex Vivo at Finite Doses ». *Skin Pharmacology and Physiology* 15 (Suppl. 1): 40-58.
558 <https://doi.org/10.1159/000066680>.

559 Egbaria, K., et N. Weiner. 1990. « Liposomes as a Topical Drug Delivery System ». *Advanced Drug*
560 *Delivery Reviews* 5 (3): 287-300. [https://doi.org/10.1016/0169-409X\(90\)90021-J](https://doi.org/10.1016/0169-409X(90)90021-J).

561 Elnaggar, Yosra, El-Massik, et Abdallah. 2011. « Fabrication, Appraisal, and Transdermal Permeation
562 of Sildenafil Citrate-Loaded Nanostructured Lipid Carriers versus Solid Lipid Nanoparticles ». *International Journal of Nanomedicine*, décembre, 3195. <https://doi.org/10.2147/IJN.S25825>.

563 Elnaggar, Yosra S.R., Magda A. El Massik, et Ossama Y. Abdallah. 2011. « Sildenafil Citrate
564 Nanoemulsion vs. Self-Nanoemulsifying Delivery Systems: Rational Development and
565 Transdermal Permeation ». *International Journal of Nanotechnology* 8 (8/9): 749.
566 <https://doi.org/10.1504/IJNT.2011.041443>.

567 « EURL ECVAM Status Report on the Development, Validation and Regulatory Acceptance of
568 Alternative Methods and Approaches (2015) ». 2015. Luxembourg: Publications Office of the
569 European Union, 2015. doi:10.2788/62058.

570 Farghali, R.A., et Rasha A. Ahmed. 2015. « Gold Nanoparticles-Modified Screen-Printed Carbon
571 Electrode for Voltammetric Determination of Sildenafil Citrate (Viagra) in Pure Form,
572 Biological and Pharmaceutical Formulations ». *International Journal of Electrochemical*
573 *Science* 10 (2): 1494-1505. [https://doi.org/10.1016/S1452-3981\(23\)05088-5](https://doi.org/10.1016/S1452-3981(23)05088-5).

574 Feldman, Henry A., Irwin Goldstein, Dimitrios G. Hatzichristou, Robert J. Krane, et John B. McKinlay.
575 1994. « Impotence and Its Medical and Psychosocial Correlates: Results of the Massachusetts
576 Male Aging Study ». *Journal of Urology* 151 (1): 54-61. [https://doi.org/10.1016/S0022-5347\(17\)34871-1](https://doi.org/10.1016/S0022-5347(17)34871-1).

577 Fink, Howard A., Roderick Mac Donald, Indulis R. Rutks, David B. Nelson, et Timothy J. Wilt. 2002.
578 « Sildenafil for Male Erectile Dysfunction: A Systematic Review and Meta-Analysis ». *Archives*
579 *of Internal Medicine* 162 (12): 1349. <https://doi.org/10.1001/archinte.162.12.1349>.

580 Gay, R., M. Swiderek, D. Nelson, et A. Ernesti. 1992. « The Living Skin Equivalent as a Model in Vitro
581 for Ranking the Toxic Potential of Dermal Irritants ». *Toxicology in Vitro* 6 (4): 303-15.
582 [https://doi.org/10.1016/0887-2333\(92\)90020-R](https://doi.org/10.1016/0887-2333(92)90020-R).

583 Ghofrani, Hossein A., Ian H. Osterloh, et Friedrich Grimminger. 2006. « Sildenafil: From Angina to
584 Erectile Dysfunction to Pulmonary Hypertension and Beyond ». *Nature Reviews Drug*
585 *Discovery* 5 (8): 689-702. <https://doi.org/10.1038/nrd2030>.

586 Guenou, Hind, Xavier Nissan, Fernando Larcher, Jessica Feteira, Gilles Lemaitre, Manoubia Saidani,
587 Marcela Del Rio, et al. 2009. « Human Embryonic Stem-Cell Derivatives for Full
588 Reconstruction of the Pluristratified Epidermis: A Preclinical Study ». *The Lancet* 374 (9703):
589 1745-53. [https://doi.org/10.1016/S0140-6736\(09\)61496-3](https://doi.org/10.1016/S0140-6736(09)61496-3).

590 Guth, Katharina, Monika Schäfer-Korting, Eric Fabian, Robert Landsiedel, et Ben van Ravenzwaay.
591 2015. « Suitability of Skin Integrity Tests for Dermal Absorption Studies in Vitro ». *Toxicology*
592 *in Vitro* 29 (1): 113-23. <https://doi.org/10.1016/j.tiv.2014.09.007>.

593 Hopf, N.B., C. Champmartin, L. Schenk, A. Berthet, L. Chedik, J.L. Du Plessis, A. Franken, et al. 2020.
594 « Reflections on the OECD Guidelines for in Vitro Skin Absorption Studies ». *Regulatory*
595 *Toxicology and Pharmacology* 117 (novembre): 104752.
596 <https://doi.org/10.1016/j.yrtph.2020.104752>.

597 Hoppel, Magdalena, Gottfried Reznicek, Hanspeter Kählig, Harald Kotisch, Günter P. Resch, et Claudia
598 Valenta. 2015. « Topical Delivery of Acetyl Hexapeptide-8 from Different Emulsions:
599 Influence of Emulsion Composition and Internal Structure ». *European Journal of*
600 *Pharmaceutical Sciences* 68 (février): 27-35. <https://doi.org/10.1016/j.ejps.2014.12.006>.

601 Huong, Srei Pisei, Hot Bun, Jean-Dominique Fourneron, Jean-Pierre Reynier, et Véronique Andrieu.
602 2009. « Use of Various Models for in Vitro Percutaneous Absorption Studies of Ultraviolet
603 Filters ». *Skin Research and Technology* 15 (3): 253-61. <https://doi.org/10.1111/j.1600-0846.2009.00368.x>.

604 Idrees, Ayesha, Inge Schmitz, Alice Zoso, Dierk Gruhn, Sandra Pacharra, Siegfried Shah, Gianluca
605 Ciardelli, Richard Viebahn, Valeria Chiono, et Jochen Salber. 2021. « Fundamental in vitro 3D
606 human skin equivalent tool development for assessing biological safety and biocompatibility

610 – towards alternative for animal experiments ». *4open* 4: 1.
611 <https://doi.org/10.1051/fopen/2021001>.

612 Iliopoulos, Fotis, Alex Chapman, et Majella E. Lane. 2021. « A Comparison of the *in Vitro* Permeation
613 of 3-O-ethyl-l-ascorbic Acid in Human Skin and in a Living Skin Equivalent (LabSkin™) ». *International Journal of Cosmetic Science* 43 (1): 107-12. <https://doi.org/10.1111/ics.12675>.

614 Kansy, Manfred, Frank Senner, et Klaus Gubernator. 1998. « Physicochemical High Throughput
615 Screening: Parallel Artificial Membrane Permeation Assay in the Description of Passive
616 Absorption Processes ». *Journal of Medicinal Chemistry* 41 (7): 1007-10.
617 <https://doi.org/10.1021/jm970530e>.

618 Kim, Tae Hwan, Soyoung Shin, Seok Won Jeong, Jong Bong Lee, et Beom Soo Shin. 2019.
619 « Physiologically Relevant In Vitro-In Vivo Correlation (IVIVC) Approach for Sildenafil with
620 Site-Dependent Dissolution ». *Pharmaceutics* 11 (6): 251.
621 <https://doi.org/10.3390/pharmaceutics11060251>.

622 Kirby, M., D. L. Creanga, et V. J. Stecher. 2013. « Erectile Function, Erection Hardness and Tolerability
623 in Men Treated with Sildenafil 100 Mg vs. 50 Mg for Erectile Dysfunction ». *International
624 Journal of Clinical Practice* 67 (10): 1034-39. <https://doi.org/10.1111/ijcp.12229>.

625 Kloner, Robert A. 2000. « Cardiovascular Risk and Sildenafil ». *The American Journal of Cardiology* 86
626 (2): 57-61. [https://doi.org/10.1016/S0002-9149\(00\)00895-X](https://doi.org/10.1016/S0002-9149(00)00895-X).

627 Kogan, Anna, et Nissim Garti. 2006. « Microemulsions as Transdermal Drug Delivery Vehicles ». *Advances in Colloid and Interface Science* 123-126 (novembre): 369-85.
628 <https://doi.org/10.1016/j.cis.2006.05.014>.

629 Kontaras, Konstantinos, Varnavas Varnavas, et Zenon S Kyriakides. 2008. « Does Sildenafil Cause
630 Myocardial Infarction or Sudden Cardiac Death? ». *American Journal of Cardiovascular Drugs*
631 8 (1): 1-7. <https://doi.org/10.2165/00129784-200808010-00001>.

632 Lane, Majella E. 2013. « Skin Penetration Enhancers ». *International Journal of Pharmaceutics* 447
633 (1-2): 12-21. <https://doi.org/10.1016/j.ijpharm.2013.02.040>.

634 Langtry, Heather D., et Anthony Markham. 1999. « Sildenafil: A Review of Its Use in Erectile
635 Dysfunction ». *Drugs* 57 (6): 967-89. <https://doi.org/10.2165/00003495-199957060-00015>.

636 Lau, Lang-Chu, et P. Ganesan Adaikan. 2006. « Mechanisms of Direct Relaxant Effect of Sildenafil,
637 Tadalafil and Vardenafil on Corpus Cavernosum ». *European Journal of Pharmacology* 541
638 (3): 184-90. <https://doi.org/10.1016/j.ejphar.2006.05.005>.

639 Lotti, Roberta, Elisabetta Palazzo, Marika Quadri, Marc Dumas, Sylvianne Schnebert, Diego Biondini,
640 Maria Anastasia Bianchini, Carine Nizard, Carlo Pincelli, et Alessandra Marconi. 2022.
641 « Isolation of an “Early” Transit Amplifying Keratinocyte Population in Human Epidermis: A
642 Role for the Low Affinity Neurotrophin Receptor CD271 ». *Stem Cells*, août, sxac060.
643 <https://doi.org/10.1093/stmcls/sxac060>.

644 Lue, Tom F., François Giuliano, Francesco Montorsi, Raymond C. Rosen, Karl-Erik Andersson, Stanley
645 Althof, George Christ, et al. 2004. « Summary of the Recommendations on Sexual
646 Dysfunctions in Men ». *The Journal of Sexual Medicine* 1 (1): 6-23.
647 <https://doi.org/10.1111/j.1743-6109.2004.10104.x>.

648 Magnano, Greta Camilla, Giovanna Marussi, Francesca Larese Filon, Matteo Crosera, Massimo
649 Bovenzi, et Gianpiero Adami. 2022. « Transdermal Permeation of Inorganic Cerium Salts in
650 Intact Human Skin ». *Toxicology in Vitro* 82 (août): 105381.
651 <https://doi.org/10.1016/j.tiv.2022.105381>.

652 Magnano, Greta Camilla, Stefania Sut, Stefano Dall’Acqua, Massimiliano Pio Di Cagno, Luke Lee, Ming
653 Lee, Francesca Larese Filon, Beatrice Perissutti, Dritan Hasa, et Dario Voinovich. 2022.
654 « Validation and Testing of a New Artificial Biomimetic Barrier for Estimation of Transdermal
655 Drug Absorption ». *International Journal of Pharmaceutics* 628 (novembre): 122266.
656 <https://doi.org/10.1016/j.ijpharm.2022.122266>.

657 Marconi, Alessandra, Marika Quadri, Annalisa Saltari, et Carlo Pincelli. 2018. « Progress in Melanoma
658 Modelling in Vitro ». *Experimental Dermatology* 27 (5): 578-86.
659 <https://doi.org/10.1111/exd.13670>.

662 Michel, Martine, Lucie Germain, Pierre Maxime Bélanger, et François A. Auger. 1995. « Functional
663 evaluation of anchored skin equivalent cultured in vitro: percutaneous absorption studies
664 and lipid analysis ». *Pharmaceutical Research* 12 (3): 455-58.
665 <https://doi.org/10.1023/A:1016277223852>.

666 Moreland, Robert B., Irwin Goldstein, et Abdulmaged Traish. 1998. « Sildenafil, a Novel Inhibitor of
667 Phosphodiesterase Type 5 in Human Corpus Cavernosum Smooth Muscle Cells ». *Life*
668 *Sciences* 62 (20): PL309-18. [https://doi.org/10.1016/S0024-3205\(98\)00158-1](https://doi.org/10.1016/S0024-3205(98)00158-1).

669 Muirhead, Gary J., David J. Rance, Donald K. Walker, et Philip Wastall. 2002. « Comparative Human
670 Pharmacokinetics and Metabolism of Single-Dose Oral and Intravenous Sildenafil: *Single-*
671 *Dose Pharmacokinetics of Sildenafil* ». *British Journal of Clinical Pharmacology* 53 (février):
672 13S-20S. <https://doi.org/10.1046/j.06-5251.2001.00028.x>.

673 Netzlaff, Frank, C.-M. Lehr, P.W. Wertz, et U.F. Schaefer. 2005. « The Human Epidermis Models
674 EpiSkin®, SkinEthic® and EpiDerm®: An Evaluation of Morphology and Their Suitability for
675 Testing Phototoxicity, Irritancy, Corrosivity, and Substance Transport ». *European Journal of*
676 *Pharmaceutics and Biopharmaceutics* 60 (2): 167-78.
677 <https://doi.org/10.1016/j.ejpb.2005.03.004>.

678 Neupane, Rabin, Sai H.S. Boddu, Jwala Renukuntla, R. Jayachandra Babu, et Amit K. Tiwari. 2020.
679 « Alternatives to Biological Skin in Permeation Studies: Current Trends and Possibilities ». *Pharmaceutics* 12 (2): 152. <https://doi.org/10.3390/pharmaceutics12020152>.

680 OECD. 2004. « Guideline for the testing of chemicals: skin absorption: in vitro method (n°428). »

681 Osman, Mohammed A., Gamal M. El Maghraby, et Mohsen A. Hedaya. 2006. « Intestinal Absorption
682 and Presystemic Disposition of Sildenafil Citrate in the Rabbit: Evidence for Site-Dependent
683 Absorptive Clearance ». *Biopharmaceutics & Drug Disposition* 27 (2): 93-102.
684 <https://doi.org/10.1002/bdd.487>.

685 Ottaviani, Giorgio, Sophie Martel, et Pierre-Alain Carrupt. 2006. « Parallel Artificial Membrane
686 Permeability Assay: A New Membrane for the Fast Prediction of Passive Human Skin
687 Permeability ». *Journal of Medicinal Chemistry* 49 (13): 3948-54.
688 <https://doi.org/10.1021/jm060230+>.

689 Otto, A., J. du Plessis, et J. W. Wiechers. 2009. « Formulation Effects of Topical Emulsions on
690 Transdermal and Dermal Delivery ». *International Journal of Cosmetic Science* 31 (1): 1-19.
691 <https://doi.org/10.1111/j.1468-2494.2008.00467.x>.

692 Ponec, Maria, Esther Boelsma, Susan Gibbs, et Mieke Mommaas. 2002. « Characterization of
693 Reconstructed Skin Models ». *Skin Pharmacology and Physiology* 15 (Suppl. 1): 4-17.
694 <https://doi.org/10.1159/000066682>.

695 Ponec, Maria, Esther Boelsma, Arij Weerheim, Aat Mulder, Joke Bouwstra, et Mieke Mommaas.
696 2000. « Lipid and Ultrastructural Characterization of Reconstructed Skin Models ». *International Journal of Pharmaceutics* 203 (1-2): 211-25. [https://doi.org/10.1016/S0378-5173\(00\)00459-2](https://doi.org/10.1016/S0378-5173(00)00459-2).

697 Rahimpour, Yahya, et Hamed Hamishehkar. 2012. « Liposomes in Cosmeceutics ». *Expert Opinion on*
698 *Drug Delivery* 9 (4): 443-55. <https://doi.org/10.1517/17425247.2012.666968>.

699 Renshall, L. J., E. C. Cottrell, E. Cowley, C. P. Sibley, P. N. Baker, E. B. Thorstensen, S. L. Greenwood,
700 M. Wareing, et M. R. Dilworth. 2020. « Antenatal Sildenafil Citrate Treatment Increases
701 Offspring Blood Pressure in the Placental-Specific *Igf2* Knockout Mouse Model of FGR ». *American Journal of Physiology-Heart and Circulatory Physiology* 318 (2): H252-63.
702 <https://doi.org/10.1152/ajpheart.00568.2019>.

703 Salonia, Andrea, Patrizio Rigatti, et Francesco Montorsi. 2003. « Sildenafil in Erectile Dysfunction: A
704 Critical Review ». *Current Medical Research and Opinion* 19 (4): 241-62.
705 <https://doi.org/10.1185/030079903125001839>.

706 Sawatdee, Somchai, Apichart Atipairin, Attawadee Sae Yoon, Teerapol Srichana, et Narumon
707 Changsan. 2019. « Enhanced Dissolution of Sildenafil Citrate as Dry Foam Tablets ». *Pharmaceutical Development and Technology* 24 (1): 1-11.
708 <https://doi.org/10.1080/10837450.2017.1281952>.

- 714 Schäfer-Korting, Monika, Udo Bock, Walter Diembeck, Hans-Jürgen Düsing, Armin Gamer, Eleonore
715 Haltner-Ukomadu, Christine Hoffmann, et al. 2008. « The Use of Reconstructed Human
716 Epidermis for Skin Absorption Testing: Results of the Validation Study ». *Alternatives to*
717 *Laboratory Animals* 36 (2): 161-87. <https://doi.org/10.1177/026119290803600207>.
- 718 Scheuplein, Robert J. 1965. « Mechanism of Percutaneous Adsorption ». *Journal of Investigative*
719 *Dermatology* 45 (5): 334-46. <https://doi.org/10.1038/jid.1965.140>.
- 720 Schmook, Fritz P., Josef G. Meingassner, et Andreas Billich. 2001. « Comparison of Human Skin or
721 Epidermis Models with Human and Animal Skin in In-Vitro Percutaneous Absorption ». *International Journal of Pharmaceutics* 215 (1-2): 51-56. [https://doi.org/10.1016/S0378-5173\(00\)00665-7](https://doi.org/10.1016/S0378-5173(00)00665-7).
- 724 Shigeta, Yasutami, Hiromichi Imanaka, Hideya Ando, Atsuko Ryu, Naoto Oku, Naomichi Baba, et
725 Taketoshi Makino. 2004. « Skin Whitening Effect of Linoleic Acid Is Enhanced by Liposomal
726 Formulations ». *Biological and Pharmaceutical Bulletin* 27 (4): 591-94.
727 <https://doi.org/10.1248/bpb.27.591>.
- 728 Simon, Gad A., et Howard I. Maibach. 2000. « The Pig as an Experimental Animal Model of
729 Percutaneous Permeation in Man: Qualitative and Quantitative Observations – An
730 Overview ». *Skin Pharmacology and Physiology* 13 (5): 229-34.
731 <https://doi.org/10.1159/000029928>.
- 732 Steinert, Peter M., et Lyuben N. Marekov. 1997. « Direct Evidence That Involucrin Is a Major Early
733 Isopeptide Cross-Linked Component of the Keratinocyte Cornified Cell Envelope ». *Journal of*
734 *Biological Chemistry* 272 (3): 2021-30. <https://doi.org/10.1074/jbc.272.3.2021>.
- 735 Steven, A.C., et P.M. Steinert. 1994. « Protein Composition of Cornified Cell Envelopes of Epidermal
736 Keratinocytes ». *Journal of Cell Science* 107 (2): 693-700.
737 <https://doi.org/10.1242/jcs.107.2.693>.
- 738 Suhail, Sana, Naseem Sardashti, Devina Jaiswal, Swetha Rudraiah, Manoj Misra, et Sangamesh G.
739 Kumber. 2019. « Engineered Skin Tissue Equivalents for Product Evaluation and Therapeutic
740 Applications ». *Biotechnology Journal* 14 (7): 1900022.
741 <https://doi.org/10.1002/biot.201900022>.
- 742 Thompson, Cecil S., Faiz H. Mumtaz, Masood A. Khan, Robert M. Wallis, Dimitri P. Mikhailidis, Robert
743 J. Morgan, Gianni D. Angelini, et Jamie Y. Jeremy. 2001. « The Effect of Sildenafil on Corpus
744 Cavernosal Smooth Muscle Relaxation and Cyclic GMP Formation in the Diabetic Rabbit ». *European Journal of Pharmacology* 425 (1): 57-64. [https://doi.org/10.1016/S0014-2999\(01\)01077-9](https://doi.org/10.1016/S0014-2999(01)01077-9).
- 747 Tracqui, A, A Miras, A Tabib, J S Raul, B Ludes, et D Malicier. 2002. « Fatal Overdosage with Sildenafil
748 Citrate (Viagra1): First Report and Review of the Literature ». *Human & Experimental*
749 *Toxicology* 21 (11): 623-29. <https://doi.org/10.1191/0960327102ht302oa>.
- 750 Tran, Diane, et Laurence Guy Howes. 2003. « Cardiovascular Safety of Sildenafil ». *Drug Safety* 26 (7):
751 453-60. <https://doi.org/10.2165/00002018-200326070-00002>.
- 752 Van Gele, Mireille, Barbara Geusens, Lieve Brochez, Reinhart Speeckaert, et Jo Lambert. 2011.
753 « Three-Dimensional Skin Models as Tools for Transdermal Drug Delivery: Challenges and
754 Limitations ». *Expert Opinion on Drug Delivery* 8 (6): 705-20.
755 <https://doi.org/10.1517/17425247.2011.568937>.
- 756 Wester, Ronald C., Joseph Melendres, Lena Sedik, Howard Maibach, et Jim E. Riviere. 1998.
757 « Percutaneous Absorption of Salicylic Acid, Theophylline, 2,4-Dimethylamine, Diethyl Hexyl
758 Phthalic Acid, Andp-Aminobenzoic Acid in the Isolated Perfused Porcine Skin Flap Compared
759 to Manin Vivo ». *Toxicology and Applied Pharmacology* 151 (1): 159-65.
760 <https://doi.org/10.1006/taap.1998.8434>.
- 761 Westmoreland, Carl, et Anthony M. Holmes. 2009. « Assuring Consumer Safety without Animals:
762 Applications for Tissue Engineering ». *Organogenesis* 5 (2): 67-72.
763 <https://doi.org/10.4161/org.5.2.9128>.

764 Wiechers, Johann W. 2005. « Optimizing Skin Delivery of Active Ingredients From Emulsions ». In
765 *Delivery System Handbook for Personal Care and Cosmetic Products*, 409-36. Elsevier.
766 <https://doi.org/10.1016/B978-081551504-3.50025-0>.
767 Williams, Adrian C, et Brian W Barry. 2004. « Penetration Enhancers ». *Advanced Drug Delivery*
768 *Reviews* 56 (5): 603-18. <https://doi.org/10.1016/j.addr.2003.10.025>.
769 Zhang, Zheng, et Bozena B. Michniak-Kohn. 2012. « Tissue Engineered Human Skin Equivalents ». *Pharmaceutics* 4 (1): 26-41. <https://doi.org/10.3390/pharmaceutics4010026>.
770 Zinner, Norman. 2007. « ORIGINAL RESEARCH—ED PHARMACOTHERAPY: Do Food and Dose Timing
771 Affect the Efficacy of Sildenafil? A Randomized Placebo-Controlled Study ». *The Journal of*
772 *Sexual Medicine* 4 (1): 137-44. <https://doi.org/10.1111/j.1743-6109.2006.00400.x>.
773 Zoio, Patrícia. 2022. « Open-source human skin model with an in vivo-like barrier for drug testing ». *ALTEX*. <https://doi.org/10.14573/altex.2111182>.
774
775
776
777
778
779